Neoplasia • Vol. 7, No. 1, January 2005, pp. 24–36

www.neoplasia.com

Grape Seed Proanthocyanidins Induce Apoptosis through p53, Bax, and Caspase 3 Pathways[1]

Anshu M. Roy, Manjeshwar S. Baliga*, Craig A. Elmets*,†,‡,§ and Santosh K. Katiyar*,†,‡,§*

Departments of *Dermatology, †Environmental Health Sciences, ‡Comprehensive Cancer Centre, University of Alabama at Birmingham, Birmingham, AL 35294, USA; §VA Medical Center, Birmingham, AL 35294, USA

Abstract

Grape seed proanthocyanidins (GSP) have been shown to inhibit skin chemical carcinogenesis and photocarcinogenesis in mice. The mechanisms responsible for the anticarcinogenic effects of GSP are not clearly understood. Here, we report that treatment of JB6 C141 cells (a well-developed cell culture model for studying tumor promotion in keratinocytes) and $p53^{+/+}$ fibroblasts with GSP resulted in a dose-dependent induction of apoptosis. GSP-induced (20–80 g/ml) apoptosis was observed by using immunofluorescence (27–90% apoptosis) and flow cytometry (18–87% apoptosis). The induction of apoptosis by GSP was p53-dependent because it occurred mainly in cells expressing wild-type p53 ($p53^{+/+}$; 15–80%) to a much greater extent than in p53-deficient cells ($p53^{-/-}$; 6–20%). GSP-induced apoptosis in JB6 C141 cells was associated with increased expression of the tumor-suppressor protein, p53, and its phosphorylation at Ser^{15}. The antiapoptotic proteins, Bcl-2 and Bcl-xl, were downregulated by GSP, whereas the expression of the pro-apoptotic protein, Bax, and the levels of cytochrome *c* release, Apaf-1, caspase-9, and cleaved caspase 3 (p19 and p17) were markedly increased in JB6 C141 cells. The downregulation of Bcl-2 and upregulation of Bax were also observed in wild-type p53 ($p53^{+/+}$) fibroblasts but was not observed in their p53-deficient counterparts. These data clearly demonstrate that GSP-induced apoptosis is p53-dependent and mediated through the Bcl-2, Bax, and caspase 3 pathways.

Neoplasia (2005) **7,** 24–36

Keywords: Apoptosis, grape seed proanthocyanidins, p53, Bcl-2, Bax, caspases, cytochrome *c*.

Introduction

Grape seeds are byproducts of grapes (*Vitis vinifera*) formed during the industrial production of grape juice and wine. They are a potent source of proanthocyanidins, which are mainly composed of dimers, trimers, and oligomers of monomeric catechins [1,2], as shown in Table 1. Grape seed proanthocyanidins (GSP) are potent antioxidants and are able to serve as free radical scavengers [3]. Their antioxidant activity is 20 times more potent than vitamin C, and 50 times more potent than vitamin E [4]. GSP has a broad spectrum of biologic activities. It is antimutagenic, anti-inflammatory, antiangiogenic, and anticarcinogenic [5–9]. It also has cytotoxic effects in diverse cancerous cell lines [10–12], which is largely mediated through apoptosis with no adverse biologic effects on the normal cells [13]. The anticarcinogenic effects of GSP on skin have been shown in 7,12-dimethylbenz(*a*)anthracene–initiated and 12-*O*-tetradecanoylphorbol-13-acetate–promoted chemical carcinogenesis in mice [14]. Recently, we have shown that dietary feeding of GSP to SKH-1 hairless mice significantly inhibited UV radiation–induced skin carcinogenesis in terms of tumor incidence, tumor multiplicity, and tumor size [6]. Dietary feeding of GSP also inhibited UV-induced malignant conversion of papillomas to carcinomas [6]. Long-term feeding of mice with GSP did not have any apparent signs of toxicity [6]. These observations indicated that GSP has a strong inhibitory effect on the tumor promotion/progression stage of multistage carcinogenesis [6,14].

p53 is a tumor-suppressor gene whose product can act as a suppressor of transformation [15] and has been shown to be induced by DNA damage [16]. In turn, p53 orchestrates a global transcriptional response that either counters cell proliferation or induces apoptosis [17]. GSP has been shown to protect against stress-induced changes in the expression of p53 and the antiapoptotic protein, Bcl-2, in human oral epithelial [18] and liver cells [3]. The Bcl-2 family of proteins consists of pro- and antiapoptotic regulators of programmed cell death/apoptosis. The established mode of action of each separate entity is to either protect or disrupt mitochondrial integrity, thereby activating or inhibiting the release of downstream

Abbreviations: Apaf-1, apoptotic protease–activating factor-1; FBS, fetal bovine serum; DMEM, Dulbecco's modified Eagle's medium; GSP, grape seed proanthocyanidins; PI, propidium iodide

Address all correspondence to: Santosh K. Katiyar, PhD, Department of Dermatology, University of Alabama at Birmingham, 1670 University Boulevard, Volker Hall 557, PO Box 202, Birmingham, AL 35294. E-mail: skatiyar@uab.edu

[1]This work was supported by funds from USPHS grants CA94593, CA105368-01 (S.K.K.), and CA79820 (C.A.E.), the Veterans Administration (18-103-02; C.A.E.), and the UAB Skin Diseases Research Center (AR050948-01).

Received 18 June 2004; Revised 27 July 2004; Accepted 27 July 2004.

DOI 10.1593/neo.04412

Table 1. Chemical Composition of GSP Used in This Study.

Constituents	Total GSP (%)
Total proanthocyanidins	89.3
Dimers	6.6
Trimers	5.0
Tetramers	2.9
Oligomers	74.8
Total monomeric flavanols	6.6
(+)-Catechin	2.5
(−)-Epicatechin	2.2
(−)-Epigallocatechin	1.4
(−)-Epigallocatechin-3-gallate	0.5
Moisture	2.2
Protein	1.1
Ash	0.8

factors such as cytochrome *c* from the mitochondrion, which stimulates apoptosis. The *Bax* gene is an apoptosis-promoting member of the *Bcl-2* gene family. The Bcl-2 protein is known to form heterodimers with the Bax protein *in vivo* and the molar ratio of Bcl-2 to Bax determines whether apoptosis is induced or inhibited in target tissues [19]. The Bax protein is considered to be one of the primary targets of p53 and controls cell death through its participation in the disruption of mitochondria with the subsequent release of cytochrome *c* [20]. Cytochrome *c* release, in turn, activates caspases 9 and 3 [21]. Cleaved caspase 3 (p17kDa and p19kDa) is regarded as a proximate mediator of apoptosis.

Inhibition of skin tumor formation in both chemical carcinogenesis and photocarcinogenesis in the skin by GSP has been associated with its chemopreventive effects during the tumor promotion stage [6,14]; however, the molecular mechanisms associated with this activity are not clearly understood. We therefore initiated studies to determine whether GSP induced apoptosis in preneoplastic epidermal keratinocytes and, if so, whether p53, the Bcl-2 family of proteins, and caspases were involved in the process. To do this, we examined the effect of GSP on the preneoplastic epidermal cell line, JB6 C141, which is a well-developed and excellent cell culture model for studying tumor promotion [22,23]. Treatment of these cells with the tumor promoter 12-*O*-tetradecanoylphorbol-13-acetate or other tumor promoters resulted in profound morphologic changes, mitogenic stimulation, and tumorigenesis in nude mice—all hallmarks of transformation to tumor cell phenotype [22,23]. Preneoplastic epidermal JB6 C141 cells have been successfully used for the determination of mechanistic pathways involving p53, Bcl-2, Bax, and caspases with chemopreventive agents [24,25]. Our data obtained from this study show that GSP induce apoptosis through their effects on p53 and several p53-dependent proteins.

Materials and Methods

Chemicals, GSP, and Antibodies

Purified GSP were obtained for this study as a generous gift from Kikkoman Corporation (Noda, Japan). The chemical composition of GSP was analyzed by Kikkoman Corporation and is given in Table 1. Dulbecco's modified Eagle's medium (DMEM), penicillin, streptomycin, fetal bovine serum (FBS), and trypsin/EDTA were purchased from CellGro (Herndon, VA). Acrylamide and the protein assay kit were obtained from Bio-Rad (Hercules, CA). Hoechst 33342 and Annexin V–conjugated Alexa Fluor 488 Apoptosis Detection Kit were purchased from Molecular Probes, Inc. (Eugene, OR). Antibodies for phospho-p53 (p53 at Ser^{15}), Bcl-xl, Bax, and cleaved caspase 3 (specific for 17 and 19 kDa) were procured from Cell Signaling Technology, Inc. (Beverley, MA). Antibodies for p53, Bcl-2, cytochrome *c*, apoptotic protease–activating factor-1 (Apaf-1), caspase 9, and β-actin were obtained from Santa Cruz Biotechnology, Inc. (Santa Cruz, CA). Enhanced chemiluminescence detection kit for Western blotting was purchased from Amersham Pharmacia Biotechnologies (Piscataway, NJ). All other chemicals employed in this study were of analytical grade and purchased from Sigma Chemical Co. (St. Louis, MO).

Cell Lines and Culture Conditions

The JB6 C141 preneoplastic mouse epidermal cell line was cultured in monolayers with DMEM supplemented with 10% (vol/vol) heat-inactivated FBS and glutamine (2 mM) at 37°C in a humidified atmosphere of 5% CO_2. $p53^{+/+}$ and $p53^{-/-}$ mouse embryonic fibroblast cells were cultured in DMEM supplemented with 15% FBS and glutamine (2 mM) at 37°C in a humidified atmosphere of 5% CO_2. For all the experiments, JB6 C141 cells, $p53^{+/+}$ fibroblast, and $p53^{-/-}$ fibroblast cells were serum-starved in 0.5% FBS/DMEM overnight and thereafter treated with GSP for 24 hours.

Cell Viability Assay

The MTT (3-[4,5-dimethylthiazol-2-yl]-2,5 diphenyltetrazolium bromide) assay was performed to determine the effect of GSP on the cellular proliferation and viability of JB6 C141, $p53^{+/+}$, and $p53^{-/-}$ cells as described previously with some modifications [26,27]. Briefly, approximately 1×10^4 cells/well were plated in 96-well plates and kept in the incubator at 37°C using previously described cell culture conditions. After overnight incubation to allow them to adhere, the cells were treated with varying concentrations of GSP (0–100 μg/ml) in fresh media for 12, 24, and 48 hours. Each treatment and time point was assayed in at least eight replicates. At the stipulated time following treatment with GSP, medium was aspirated and MTT (50 μl of a 5 mg/ml stock solution in PBS) was added in each well of the 96-well culture plate. Incubation was continued at 37°C for an additional 2 hours. At that time, the plates were spun, supernatants were discarded, and purple-colored precipitates of formazan were dissolved in 150 μl of dimethyl sulfoxide. The color absorbance of each aliquot was recorded at 540 nm with a Bio-Rad 3350 microplate reader with a reference at 650 nm serving as a blank. The reduction in viability of cells in each well was expressed as the percentage compared to non–GSP-treated control cells.

Detection of Apoptotic Cells by Immunofluorescence Staining

Cells were treated for 24 hours with GSP (20–80 μg/ml) and were then washed with PBS, after which they were fixed in freshly prepared 0.1% ice-cold paraformaldehyde for 10 minutes. The cells were then washed twice with PBS and stained with Hoechst 33342 (50 μg/ml) for 1 minute in the dark. Morphologic changes were observed using fluorescent microscopy in a blinded manner, the percentage of apoptotic cells was scored by counting at least 200 cells per treatment group, and the average percentage of apoptotic cells was determined for each treatment group. The experiment was repeated at least three times.

Quantification of Apoptotic Cells by Flow Cytometry

Induction of apoptosis by GSP treatment was further quantified using the Annexin V–Alexa Fluor 488 Apoptosis Detection kit following the manufacturer's protocol. Briefly, JB6 C141 cells, $p53^{+/+}$ fibroblast, or $p53^{-/-}$ fibroblast cells were treated with GSP (20–80 μg/ml) or without GSP for 24 hours. Cells were harvested, washed with cold PBS, and subjected to Annexin V and propidium iodide (PI) staining in binding buffer at room temperature for 15 minutes in the dark. Stained cells were analyzed by fluorescence-activated cell sorting (FACSCalibur; BD Biosciences, San Jose, CA) using CellQuest 3.3 Software. In this apoptotic assay kit, recombinant Annexin V conjugated to Alexa Fluor 488 fluorescent dye was used, which enhanced its sensitivity. The apoptotic cells stained with Annexin V showed green fluorescence and were present in the lower right (LR) quadrant of the histogram. The cells stained with both Annexin V and PI showed red and green fluorescence, and were present in the upper right (UR) quadrant of the FACS histogram.

Preparation of Cell Lysates, Immunoprecipitation, and Western Blotting

Following treatment of JB6 C141, $p53^{+/+}$ or $p53^{-/-}$ fibroblasts were incubated with or without GSP at the required concentrations for 24 hours. The cells were harvested, washed twice with cold PBS (10 mM, pH 7.4) and lysed with ice-cold lysis buffer (50 mM Tris–HCl, 150 nM NaCl, 1 mM EGTA, 1 mM EDTA, 1% NP-40, 1 mM sodium orthovanadate, 20 mM NaF, 1 mM PMSF, 10 μg/ml aprotinin, and 10 μg/ml leupeptin, pH 7.4) for half an hour over ice, as described previously [28]. The lysate was then collected in a microfuge tube and passed through a 21-gauge needle to break up the cell aggregates. The lysate was cleared by centrifugation at 14,000 rpm for 10 minutes at 4°C and the supernatant was used for Western blot analysis at that time or was stored at −80°C for future use. The lysates containing 200 μg of protein were immunoprecipitated using a monoclonal mouse IgG antibody against p53 and rotated overnight at 10 cycles/min at 4°C. Thereafter, protein A/G plus agarose beads were added and continuously rotated for another 3 hours at 4°C. The beads were washed three times with PBS and were examined for phosphorylated p53 protein (Ser^{15}). The protein concentration was determined by the DC Bio-Rad assay using the manufacturer's protocol. For Western blot analysis, proteins (30–50 μg) were resolved on 10–14% sodium dodecyl sulfate polyacrylamide gel and transferred onto a nitrocellulose membrane. The membranes were treated with blocking buffer (5% nonfat dry milk in 0.1% Tween 20 in 20 mM Tris-buffered saline, pH 7.5) by incubating them for 1 hour at room temperature. This was followed by incubation with the appropriate primary antibody (at the dilutions recommended by the manufacturer) in blocking buffer overnight at 4°C. The blot was then washed with PBS and then was incubated with the appropriate secondary antibody conjugated with horseradish peroxidase at room temperature for 1 hour. Protein bands were then visualized using the ECL detection system (Amersham Life Science, Inc., Piscataway, NJ). Autoradiography was performed with XAR-5 film (Eastman Kodak Co., Rochester, NY). To verify equal protein loading and transfer, the blots were stripped and reprobed for β-actin using an antiactin rabbit polyclonal antibody and, thereafter, the same protocol was followed as detailed above. To compare the relative intensity of each protein band from different groups in Western blot, computerized densitometry was performed using OPTIMAS 6.2 software program.

Statistical Analysis

The Student's *t* test was performed to determine the statistical significance of the difference in the absolute values of the apoptotic cell death between the GSP-treated and non–GSP-treated groups. The GSP-induced apoptosis was considered significant at $P < .05$ where not mentioned.

Results

GSP Treatment Decreases Cell Viability in JB6 C141 Cells

A preliminary screening test was performed to assess the effect of GSP on cellular proliferation and viability at different time points using the MTT assay. As shown in Figure 1, there was a dose- and time course–dependent reduction in the viability of JB6 C141 cells treated with GSP (20–80 μg/ml). Treatment with GSP for 12 hours did not result in a significant

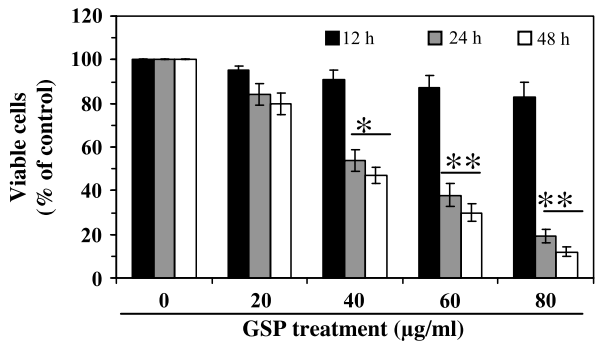

Figure 1. *GSP inhibits the proliferation and cell viability of preneoplastic epidermal JB6 C141 cells in a dose-dependent manner. Dose-dependent effect of GSP on the viability of JB6 C141 cells was determined by the MTT assay as described in the Materials and Methods section. Data are presented in terms of the mean ± SD of eight replicates. *P < .01 vs control (non-GSP); **P < .001 vs control (non-GSP).*

reduction in cell viability, whereas with 24 hours of treatment, a significant reduction in cell viability (16–81%, $P < .01$–.001) was observed. The cell viability decreased even further when cells were incubated with GSP for 48 hours (20–88%). Because the cell viability of JB6 C141 cells was significantly decreased by GSP after 24 hours of its treatment, we selected this particular time point for further studies.

GSP Treatment Induces Apoptosis in JB6 C141 Cells

To determine the effect of GSP treatment on the induction of apoptosis in JB6 C141 cells, immunofluorescence staining was performed to detect the number of apoptotic cells (Figure 2). At doses of 20, 40, 60, and 80 μg/ml GSP, a significant increase in apoptosis of JB6 C141 cells was observed, which ranged from 21% to 90% ($P < .01$–.001). We further confirmed our observations using flow cytometry. In this assay, cells were stained with Annexin V–conjugated Alexa Fluor 488 dye (which was used to detect apoptotic cells with externalized phosphatidyl-serine leaflets) and PI. The cells in the lower right quadrant of the histogram (LR; Figure 3) represent the number of early apoptotic cells. Those in the upper right (UR; Figure 3) quadrant represented the cells in late apoptosis, which had taken up both Alexa Fluor 488 and PI [25,27]. We found that treatment with GSP (20–80 μg/ml) for 24 hours increased the number of early apoptotic cells from 9.5% to 15.4% in a dose-dependent manner compared to only 2.8% of early apoptotic cells in the non–GSP-treated (control) group. The number of late apoptotic cells (in UR quadrant) also increased from 4.3% in the untreated control group to 71.9% at the highest GSP dose level (80 μg/ml). The total percentage of apoptotic cells (UR + LR) increased from 7.1% in the control group to 87.3% with 80 μg/ml GSP treatment.

GSP Treatment Upregulates p53 Expression with a Concomitant Increase in Phosphorylation of p53 in JB6 C141 Cells

p53 protein plays a pivotal role in the suppression of transformation [15]. Activation of p53 tumor-suppressor functions is critically dependent on the phosphorylation at the Ser^{15} residue [29]. To determine the role of p53 in the induction of apoptosis by GSP treatment in JB6 C141 cells, which express wild-type p53, we assessed total p53 protein levels and phosphorylated p53 at Ser^{15} by Western blot analysis. We observed a significant increase in the basal level of p53 protein (Figure 4, *upper panel*) as well as a concomitant increase in its phosphorylation (Figure 4, *lower panel*) in a dose-dependent manner with GSP treatment (20–80 μg/ml). The increase in p53 after GSP treatment may be because of its stability and/or activation.

p53-Deficient ($p53^{-/-}$) Cells Are Resistant to GSP-Induced Apoptosis

Similar to JB6 C141 cells, the effect of GSP on cell viability of $p53^{+/+}$ and $p53^{-/-}$ cells was determined using MTT assay. There was no significant inhibition in cell viability of $p53^{+/+}$ and $p53^{-/-}$ cells observed after 12 hours of GSP treatment. However, treatment of GSP at doses of 20, 40,

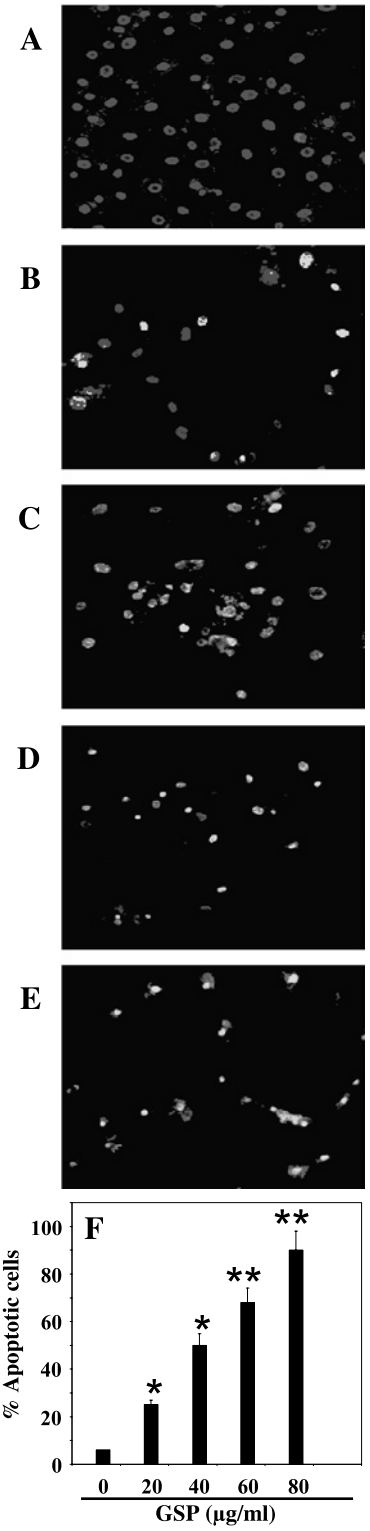

Figure 2. *GSP induces apoptosis in JB6 C141 cells. Apoptosis was determined by immunofluorescence staining as detailed in the Materials and Methods section. Briefly, cells were treated with GSP for 24 hours; thereafter, morphologic changes in JB6 C141 cells undergoing apoptosis were observed under fluorescence microscopy. Cells were treated without GSP (panel A) and with GSP (panels B, C, D, and E for 20, 40, 60, and 80 μg/ml, respectively) for 24 hours after overnight serum starvation. The number of apoptotic cells induced with or without GSP treatment is summarized in panel F. The experiment was repeated two times and the average percentage of apoptotic cells ± SD for each treatment group is indicated. At least 200 cells were counted in a blinded manner to score the percentage of apoptosis in each treatment group. *P < .01 vs control (non-GSP); **P < .001 vs control (non-GSP).*

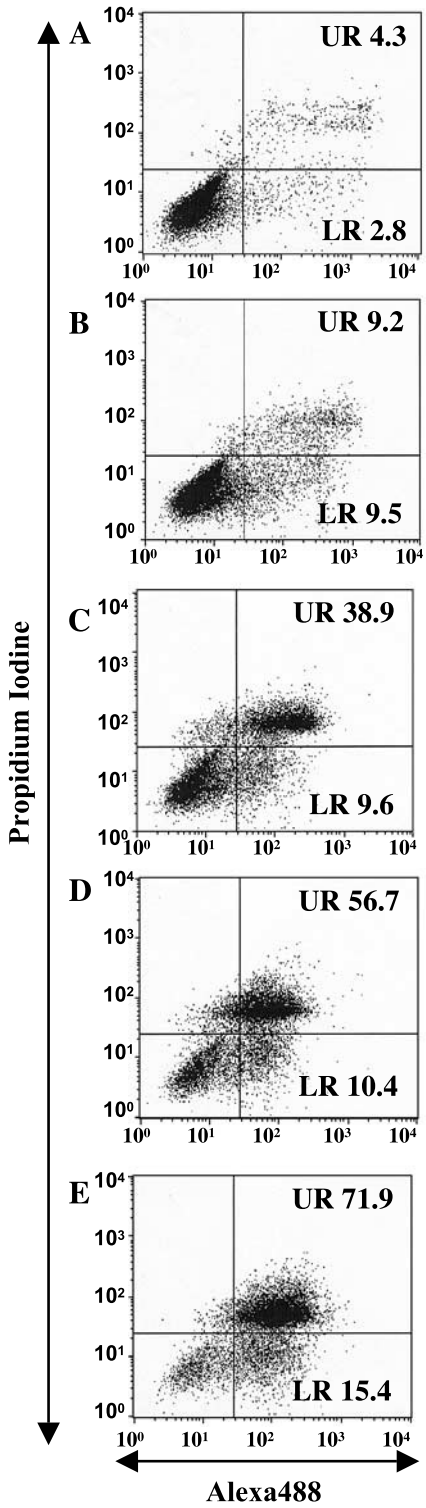

Figure 3. *GSP-induced apoptosis in JB6 C141 cells was determined by the flow cytometry using Annexin V–Alexa Fluor 488 Apoptosis Vybrant Assay kit. Cells were incubated with Annexin V–conjugated Alexa Fluor 488 and PI in binding buffer at room temperature following the manufacturer's protocol. Panel A indicates the control cells (non-GSP treatment). The cells in panels B, C, D, and E were treated with 20, 40, 60, and 80 μg/ml GSP for 24 hours after overnight serum starvation as detailed in Materials and Methods section. LR (lower right) quadrant depicts the percentage of early apoptotic cells (Annexin V–stained cells) and the UR (upper right) quadrant depicts the percentage of late apoptotic cells (Annexin V+PI–stained cells).*

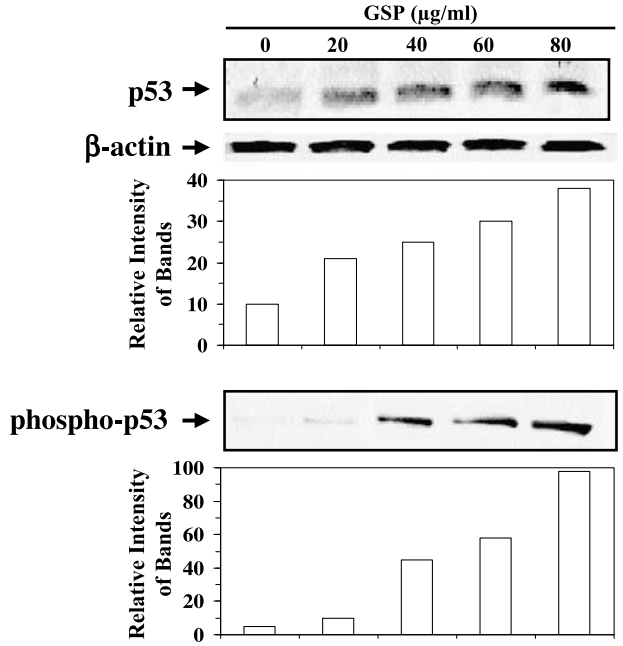

Figure 4. *GSP increases p53 level and induces phosphorylation of p53 at Ser[15] in JB6 C141 cells. Serum-starved JB6 C141 cells were treated with varying doses of GSP (20–80 μg/ml) for 24 hours. Cell lysates were prepared from these cells, and 200 μg of proteins was used for immunoprecipitation to detect the phosphorylation of p53 at Ser[15] using a specific antibody, as described in Materials and Methods section. The same blot was stripped and reprobed using an antibody against total p53. β-Actin was used as an internal control to monitor the equal loading and transfer of proteins from gels to membranes. Relative intensity of the bands was determined and is shown below the blots. Experiments were repeated three times and a representative blot is shown.*

60, and 80 μg/ml to $p53^{+/+}$ cells for 24 hours resulted in a dose-dependent inhibition of cell viability (14 ± 4% to 76 ± 8%) compared to that of non–GSP-treated control cells. The cell viability of $p53^{+/+}$ cells was further decreased after 48 hours of GSP treatment (20–84%). In contrast, the inhibition of cell viability in p53-deficient ($p53^{-/-}$) cells was not as much as in $p53^{+/+}$ cells with GSP (20–80 μg/ml) treatment after 12, 24, or 48 hours. The inhibition of cell viability in $p53^{-/-}$ cells ranged from 6% to 16%.

To obtain more definitive evidence that p53 is required for the induction of apoptosis by GSP, the effect of GSP on a fibroblast cell line derived from p53-deficient ($p53^{-/-}$) mouse embryos and their wild-type $p53^{+/+}$ counterpart was examined. $p53^{+/+}$ (wild-type) cells treated with increasing doses of GSP exhibited a dose-dependent increase in the number of cells undergoing apoptosis, which ranged from 35% to 79% compared to 15% in non–GSP control cells, as detected by morphologic methodology (Figure 5, *panels A–E*). The degree to which $p53^{+/+}$ fibroblasts underwent apoptosis was further quantitated by flow cytometry. The number of cells in the GSP-induced early phase of apoptosis ranged from 29.3% to 52.7% after 24 hours of GSP treatment compared to only 18.9% in the non–GSP-treated group. Similarly, there was a dose-dependent increase in cells in the late phase (UR) of apoptosis. The total number of cells undergoing apoptosis after GSP treatment was 33.2% to 77.9% compared to 22.9% in the non-GSP control group.

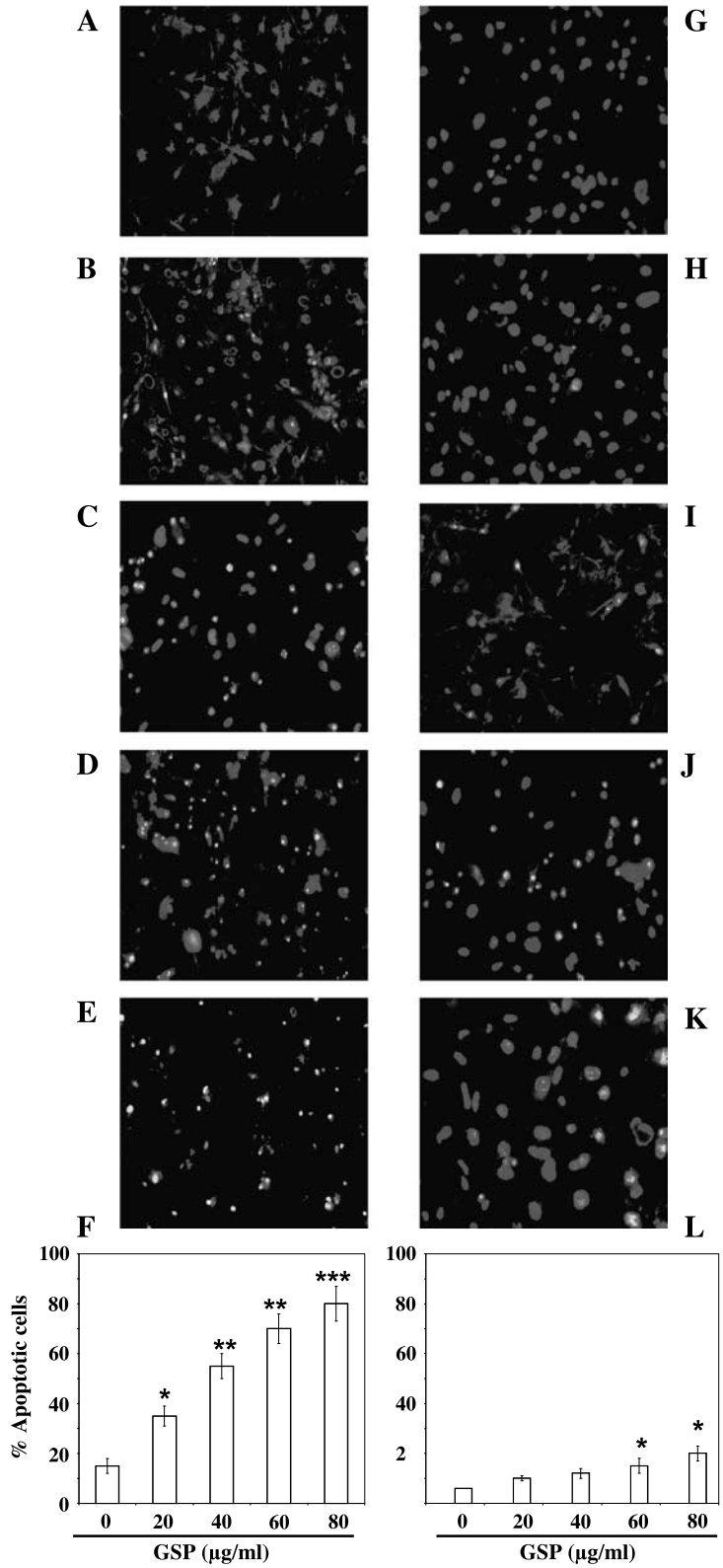

Figure 5. *GSP induces significantly less apoptosis in p53-deficient ($p53^{-/-}$) cells compared to p53 wild-type ($p53^{+/+}$) cells. Both $p53^{+/+}$ and $p53^{-/-}$ fibroblast cells were cultured under identical conditions as was done in JB6 C141 cells except that the cells were treated with 15% FBS in DMEM. Cells were starved in 0.5% FBS/DMEM overnight and thereafter treated with GSP in serum-containing media for another 24 hours. Morphologic changes in $p53^{+/+}$ and $p53^{-/-}$ fibroblast cells undergoing apoptosis were observed under fluorescence microscopy. Cells in panels A and G were not treated with GSP (controls), whereas increasing concentrations of GSP were added to cultures for 24 hours after overnight serum starvation in panels B–E and H–K by 20, 40, 60, and 80 μg/ml, respectively. The percentage of apoptotic cells from panel A to panel E is summarized in panel F, and the percentage of apoptotic cells from panel G to panel K is summarized in panel L. The experiment was repeated at least two times and the average percentage of apoptotic cells ± SD for each treatment group is indicated. At least 200 cells were counted in a blinded manner to score the percentage of apoptosis in each treatment group. *P < .01 vs control (non-GSP); **P < .005 vs control (non-GSP); ***P < .001 vs control (non-GSP).*

Having ascertained that $p53^{+/+}$ fibroblasts responded to GSP in a manner that was similar to JB6 C141 cells, we evaluated the effect of treatment with GSP on the p53-deficient ($p53^{-/-}$) fibroblast cell line. At none of the dose levels employed did $p53^{-/-}$ achieve a level of apoptosis that was comparable to that seen in the $p53^{+/+}$ counterparts (Figure 5). It should be noted that $p53^{-/-}$ fibroblasts did undergo some apoptosis at the two highest treatment levels (60 and 80 μg/ml) (Figure 5, *panels J and K*), but even at these doses, the level of apoptosis was not nearly as great as in the $p53^{+/+}$ fibroblasts. The resistance of $p53^{-/-}$ cells to apoptosis by GSP was confirmed by flow cytometry (Figure 6, *panels F–J*). The percentage of cells undergoing early (LR quadrants) and late (UR quadrants) apoptosis was increased only at the 60 and 80 μg/ml GSP doses. The total number of apoptotic cells was only 17.4% at the maximum dose of GSP (80 μg/ml), which is significantly less than that induced by GSP in the $p53^{+/+}$ cells (77.9%, $P < .005$).

GSP Treatment Downregulates Antiapoptotic Proteins, Bcl-2 and Bcl-xl, with a Concomitant Increase in Pro-Apoptotic Protein, Bax, in JB6 C141 Cells

The Bcl-2 and Bcl-xl proteins inhibit programmed cell death and are associated with cell survival. Their expression corresponds with the p53 status of the cells. Bax is another pro-apoptotic member of this family, which increases apoptosis in cells [19,30,31]. We therefore reasoned that if p53 was involved in GSP-induced apoptosis, there would be decreased expression of Bcl-2 and Bcl-xl and increased expression of Bax proteins in GSP-treated JB6 C141 cells. Compared with control non–GSP-treated cells, treatment of JB6 C141 cells with GSP resulted in a dose-dependent decrease in the levels of Bcl-2 expression. GSP treatment at the 60 and 80 μg/ml doses resulted in >90% inhibition of Bcl-2 (Figure 7, *panel A*). GSP treatment also induced a dose-dependent reduction in the levels of Bcl-xl protein, with nearly 100% inhibition at the 80 μg/ml GSP dose (Figure 7, *panel D*). The level of pro-apoptotic Bax protein was correspondingly upregulated from 1.3- to 3.1-fold with increasing doses of GSP (Figure 7, *panel B*). Importantly, the ratio of Bax/Bcl-2 protein expression after GSP treatment was dose-dependently increased by several folds (panel C), which indicated the susceptibility of JB6 C141 cells toward undergoing apoptosis.

GSP Treatment Induces Cytochrome c Release, Induction of Apaf-1, and Activation of Caspases in JB6 C141 Cells

Cellular apoptosis may involve the disruption of mitochondrial function through the release of cytochrome *c* from mitochondria into the cytosol. Cytosolic cytochrome *c* can bind to Apaf-1 and activate caspase 9 in the apoptosome in response to diverse inducers of cell death, which may lead to the activation of caspase-3, which subsequently leads to apoptosis [32–34]. For better understanding and an insight on the role of these proteins, we determined whether induction of apoptosis in JB6 C141 cells by GSP is associated with disruption of mitochondrial function and activation of caspases. Treatment of JB6 C141 cells with GSP (20–80 μg/ml) resulted in a dose-dependent increase in cytochrome *c* release from mitochondria (Figure 8, *panel A*), induction of Apaf-1 (Figure 8, *panel B*), and activation of caspase 9 (Figure 8, *panel C*) and caspase 3 (Figure 8, *panel D*) compared to non–GSP-treated control cells. Activated or cleaved caspase-3 (17 and 19 kDa) is considered as one of the key executioners of apoptosis. Because cleaved caspase 3 antibody only recognizes the cleaved products of caspase 3 (17 and 19 kDa), the original basal level of uncleaved caspase 3 was not detected in the blot.

GSP Treatment Downregulates Antiapoptotic Protein, Bcl-2, and Concomitantly Increases Pro-Apoptotic Protein, Bax, in $p53^{+/+}$ Cells But Not in $p53^{-/-}$ Cells

Finally, we determined whether there was a difference in Bcl-2, Bcl-xl, and Bax proteins on GSP-induced apoptosis when $p53^{+/+}$ and $p53^{-/-}$ fibroblast cells were compared. Treatment of GSP decreased the expression of Bcl-2 (4–60%) in $p53^{+/+}$ cells (Figure 9, *left, panel A*) but had virtually no effect in p53-deficient cells ($p53^{-/-}$) (Figure 9, *right, panel E*). In contrast to the effects on Bcl-2, Bcl-xl protein levels were similar in the GSP-treated $p53^{+/+}$ (*left, panel D*) and the $p53^{-/-}$ (*right, panel H*) cells. The lack of an effect of p53 on Bcl-xl may be the reason why some $p53^{-/-}$ cells underwent apoptosis when higher GSP doses were given (Figures 5 and 6). Treatment with GSP, which increased the expression of Bax protein in the $p53^{+/+}$ cells (Figure 9, *left, panel B*), had no effects on its expression in $p53^{-/-}$ cells (Figure 9, *right, panel F*). It is important to mention that the ratio of Bax/Bcl-2 proteins is critical for apoptosis signal. Here, we found that the ratio of Bax/Bcl-2 was increased by about four-fold in GSP-treated $p53^{+/+}$ cells compared to non–GSP-treated $p53^{+/+}$ cells (Figure 9, *panel C*). However, the Bax/Bcl-2 ratio was almost unaffected after GSP treatment in $p53^{-/-}$ cells (Figure 9, *panel G*). These observations indicate that p53 may have a role in regulating the expression of Bcl-2 and Bax proteins after GSP treatment.

Discussion

Chemoprevention is a promising strategy used to control the occurrence of cancer. Several botanicals and/or dietary supplements have been shown to have anticarcinogenic properties. GSP is one of such dietary botanical supplement, which has recently been shown to have these properties [6–12,14]. *In vivo* animal experiments have shown that proanthocyanidins from grape seeds possess potent chemopreventive effects against the development of skin tumors [6,14]. However, the molecular mechanisms of anticarcinogenic effects in skin are not clearly understood. Ideally, the chemopreventive agents should be nontoxic and relatively free of side effects, so they can be administered to healthy people for long periods of time. We have shown that long-term dietary feeding of GSP to animals did not induce apparent signs of toxicity [6]. GSP has been shown to have anticancer or cytotoxic activity in *in vitro* tumor cells [7–13] and *in vivo* animal models [6,14,35], while

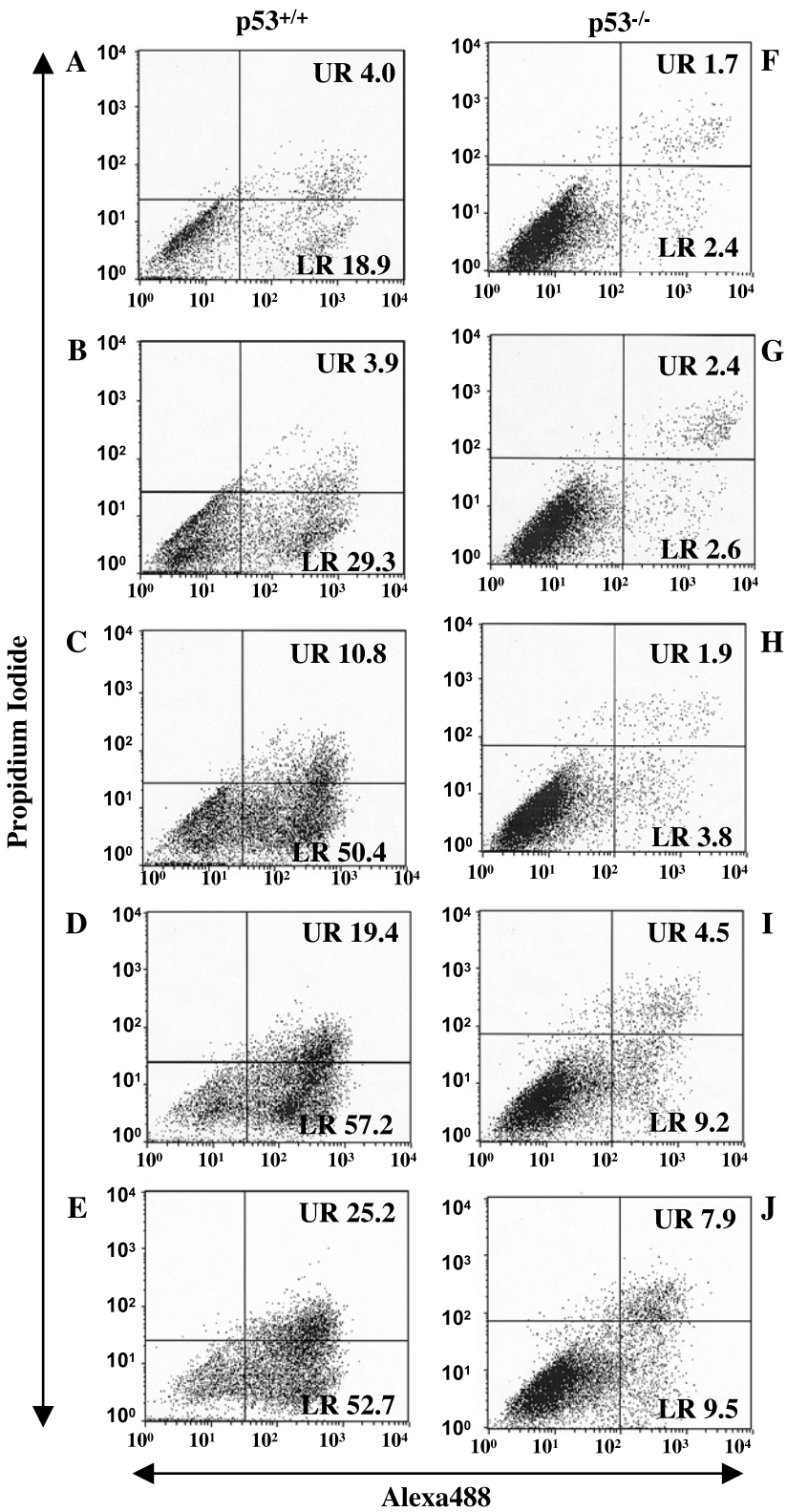

Figure 6. *GSP induces significantly less apoptosis in p53-deficient cells ($p53^{-/-}$) than in p53 wild-type ($p53^{+/+}$) cells as detected by FACS analysis. Both $p53^{+/+}$ and $p53^{-/-}$ fibroblast cells were cultured in conditions that were identical to those described in Figure 5 and Materials and Methods section. Cells in panels A and F were not treated with GSP (controls), whereas cells in panels B–E and G–J were given increasing concentrations of GSP (B–E and G–J by 20, 40, 60, and 80 μg/ml, respectively) for 24 hours after overnight serum starvation. The percentage of apoptotic cells was determined by the Annexin V–Alexa Fluor 488 Apoptosis Vybrant Assay kit following the manufacturer's protocol. The lower right (LR) quadrant depicts the percentage of early apoptotic cells (Annexin V–stained cells) and the upper right (UR) quadrant depicts the percentage of late apoptotic cells (Annexin V+PI–stained cells).*

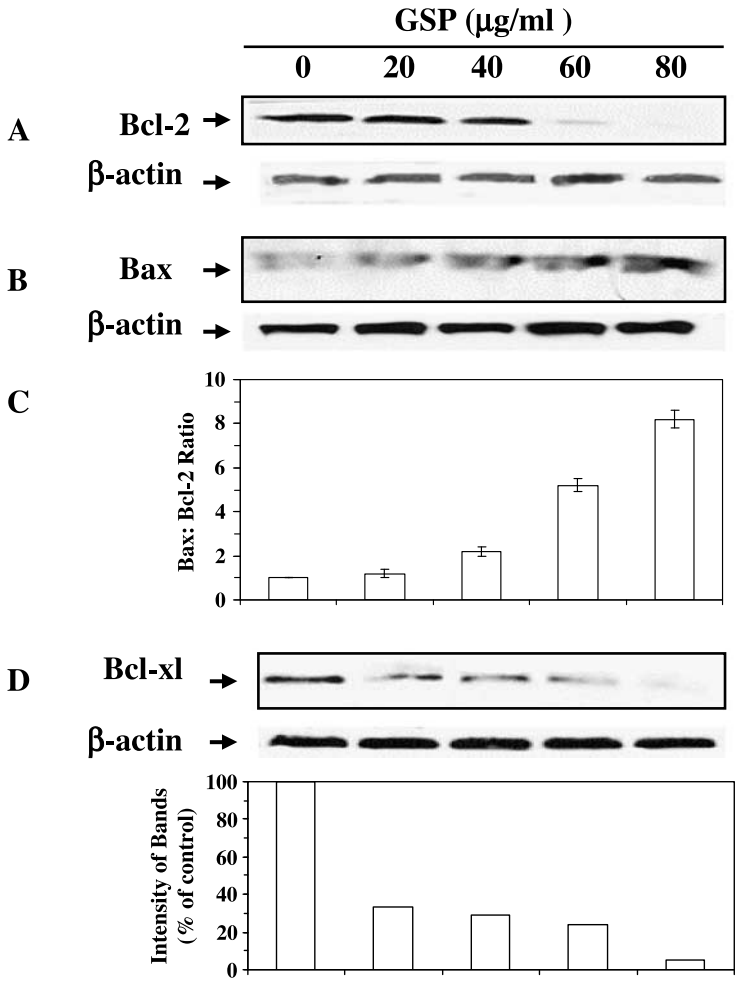

Figure 7. *Treatment of GSP decreases the expression of the antiapoptotic proteins, Bcl-2 and Bcl-xl, and increases the expression of the pro-apoptotic protein, Bax, in JB6 C141 cells. JB6 C141 cells were starved in 0.5% FBS/DMEM overnight and then treated with GSP (20–80 μg/ml) in serum-containing media for another 24 hours. Cell lysates were prepared, and the expression of the proteins was determined by Western blot analysis using the corresponding antibodies, as detailed in the Materials and Methods section. Relative intensity of bands in each panel was determined. GSP treatment to JB6 C141 cells decreased the expressions of the antiapoptotic proteins, Bcl-2 (panel A) and Bcl-xl (panel D), whereas the expression of the pro-apoptotic protein, Bax, was increased (panel B). A representative blot is shown from three independent experiments with identical results. The ratio of Bax and Bcl-2 protein expression was determined from three separate experiments by comparing the relative intensities of protein bands and shown as a mean ± SD (panel C). β-Actin was used as an internal control to monitor equal protein loading and transfer of proteins from the gel to the membranes after stripping them and reprobing them with the actin antibody.*

enhancing the growth and viability of the normal cells [13]. In this study, we found that treatment of GSP resulted in a reduction of cell viability (Figure 1) and induction of apoptosis in JB6 C141 cells (Figures 2 and 3). Inhibition of apoptosis is considered as one of the possible mechanisms of tumor development and many chemopreventive agents have been shown to act through the induction of apoptosis to inhibit or block the carcinogenic process [36–38]. Therefore, our data indicated that the induction of apoptosis may be one of the mechanisms for the anticarcinogenic effect of GSP. Moreover, a large volume of evidence indicates that apoptosis may represent a protective mechanism against neoplastic development by eliminating genetically damaged cells or excess cells that have improperly been induced to proliferate by factors such as carcinogens [39,40].

Normal p53 has been shown to exert its tumor-suppressing activity by regulating the process of apoptosis [41,42]. This fact was supported by the findings that *p53* is the most commonly mutated tumor-suppressor gene, and that lack of p53 expression or function is associated with an increased risk of tumor formation [43,44]. To investigate the possible role of p53 in the induction of apoptosis by GSP, we determined the effect of GSP on JB6 C141 cells and in $p53^{+/+}$ and $p53^{-/-}$ cell lines. It is evident from our data that the levels of p53 and its activated/phosphorylated form were upregulated after GSP treatment and that the induction of apoptosis by GSP is mediated through this protein. Phosphorylation of p53 has been associated with cellular damage occurring during anticancer therapy [45]. p53 phosphorylation at Ser^{15} increases its half-life and thus increases the accumulation and functional activation of p53 in response to DNA damage, thereby stabilizing it [46,47]. This information provides evidence that increase in p53 protein expression after GSP treatment may be due to increased stability. To additionally confirm that p53 is involved in GSP-induced apoptosis, we compared the effect of GSP in wild-type p53

fibroblast cells ($p53^{+/+}$) and p53-deficient fibroblast cells ($p53^{-/-}$). Our results showed that treatment of GSP significantly induced apoptosis in $p53^{+/+}$ cells, whereas $p53^{-/-}$ cells failed to respond to GSP with the significant induction of apoptosis (Figures 5 and 6). These results provide definitive evidence for the requirement of p53 in GSP-induced apoptosis. Loss of tumor-suppressor gene function has been correlated with amelioration of apoptosis and enhanced growth of tumors [48]. Conversely, Kaina [49] has mentioned that mouse fibroblasts deficient for p53 were more sensitive to induction of apoptosis due to the direct involvement of p53 in DNA repair and attributed the apoptotic

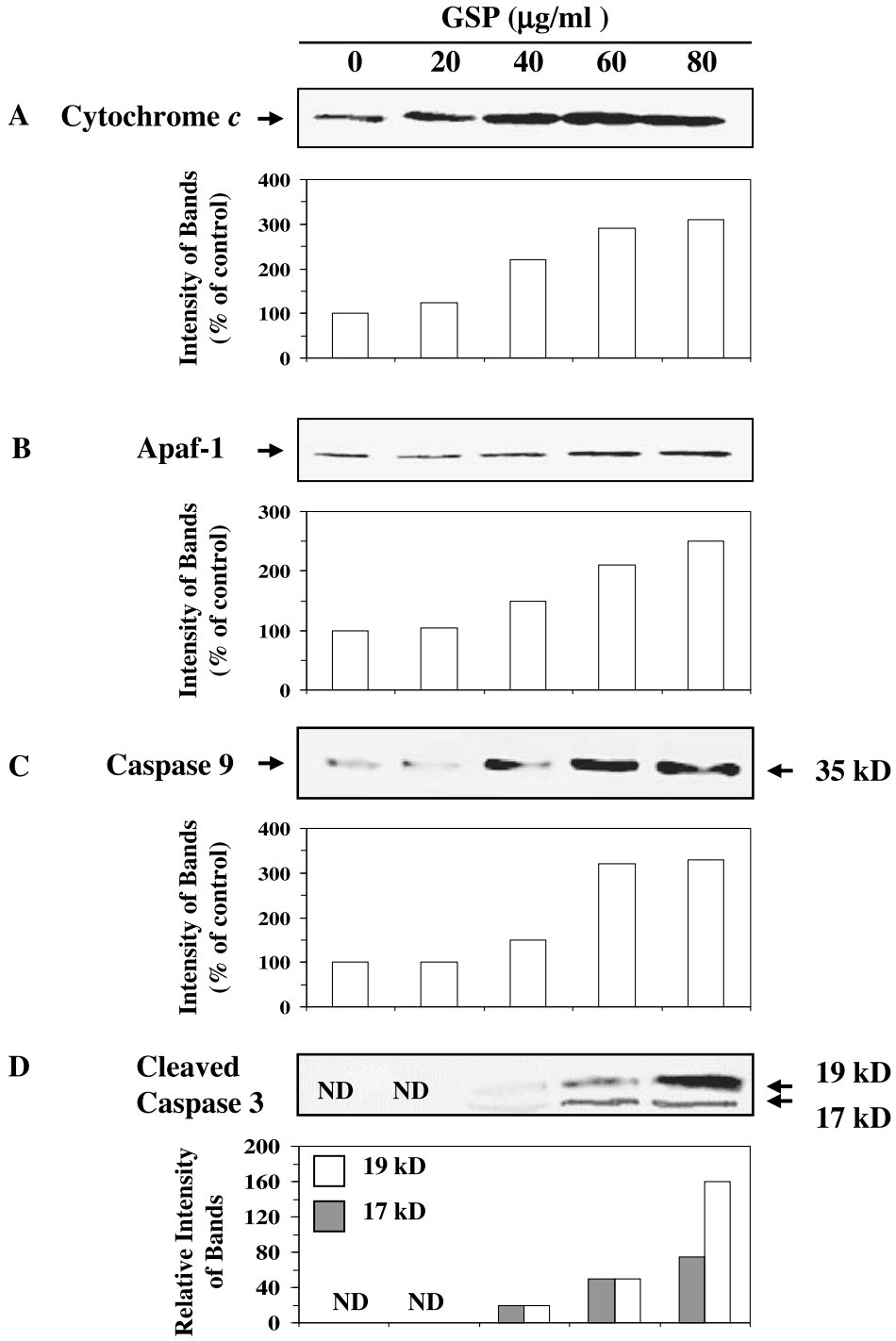

Figure 8. *Treatment of GSP increases the release of cytochrome c (panel A) and increases the expression of apoptotic protease–activating factor-1 (Apaf-1; panel B), caspase 9 (panel C), and cleaved caspase 3 (panel D) in JB6 C141 cells. Antibody for caspase 3 specifically recognizes the cleaved products of caspase 3 (19 and 17 kDa), whereas the antibody for caspase 9 recognizes the cleaved (active) product at 35 kDa. A representative blot is shown from three independent experiments with identical results. Cells were cultured and treatments were performed as described in Figure 4, and protein levels were analyzed by Western blot analysis as described in the Materials and Methods section. Relative intensity of bands in each panel was determined and shown below each respective panel. ND = not detectable.*

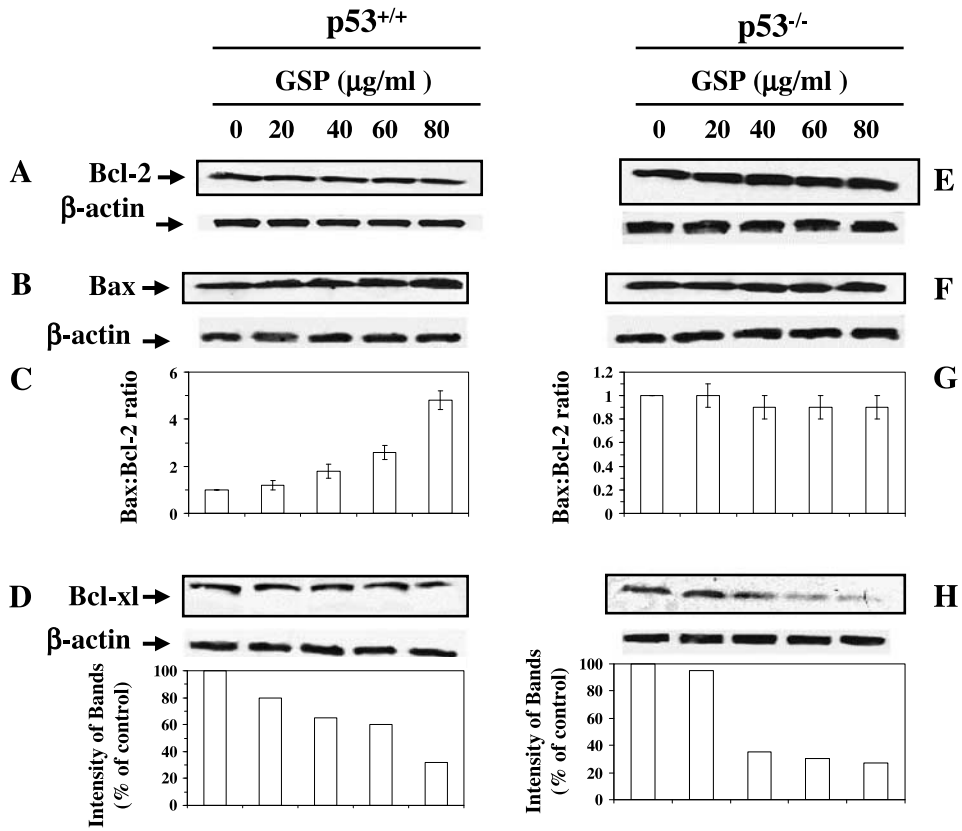

Figure 9. *Treatment of GSP decreases the expression of antiapoptotic proteins, Bcl-2 and Bcl-xl, and increases the expression of pro-apoptotic protein, Bax, in p53$^{+/+}$ cells (left, panels A, B, and D). In p53-deficient cells (right panels), however, the levels of Bcl-2 (panel E) and Bax (panel F) remain almost unchanged. In contrast, GSP also decreases Bcl-xl expression in p53$^{-/-}$ (panel H). A representative blot is shown from three independent experiments with identical results. The ratio of Bax and Bcl-2 protein expression in p53$^{+/+}$ and p53$^{-/-}$ fibroblasts was determined from three separate experiments and shown as mean ± SD (panels C and G). Cells were cultured as described in Figure 5. After treatment with GSP for 24 hours, cells were harvested, lysates were prepared, and protein levels were analyzed by Western blot analysis as described in the Materials and Methods section. β-Actin was used as an internal control to monitor equal loading of the proteins.*

pathway to be dependent on the cell type. Our results as well as the data of others with resveratrol [24] and caffeine [25], however, also indicate that the probability of the induction of apoptosis through the p53 pathway is dependent both on the cell type and the ability of the agent being tested to induce apoptosis.

Experimental evidence suggests that several pathways mediate p53-induced apoptosis, and one of these involves the Bax protein. Bax is a p53 target and a proapoptotic member of the Bcl-2 family of proteins [50,51]. The Bcl-2 family consists of both pro- and antiapoptotic members that elicit opposing effects on mitochondria. Transcriptional activation by p53 of pro-apoptotic Bax can enhance the permeability of the mitochondrial membrane, which in turn results in the release of apoptogenic factors. Repression of antiapoptotic members such as Bcl-2 and Bcl-xl, which are transcriptionally suppressed by p53 [52], preserves the integrity of the mitochondria. This blocks the release of these soluble intermembrane factors, such as cytochrome *c*, that activate the effectors of apoptosis [53]. In this study, we have shown that GSP upregulates the pro-apoptotic Bax protein and downregulates the antiapoptotic protein Bcl-2 in JB6 cells (Figure 7) and p53$^{+/+}$ fibroblasts (Figure 9), but does not do so in p53$^{-/-}$ cells (Figure 9). More importantly, the ratio of Bax/Bcl-2 protein expression is critical for apoptosis, and the ratio of Bax/Bcl-2 dictates a cell's susceptibility to undergo apoptosis under experimental conditions [54–56]. Alteration in the Bax/Bcl-2 ratio causes the release of cytochrome *c* from mitochondria into cytosol. Cytosolic cytochrome *c* can bind to Apaf-1 and activate caspase 9 in the apoptosomes in response to diverse inducers of cell death [32–34]. Activation of caspase 9 leads to the activation of caspase 3, which is one of the key mediators of p53-induced apoptosis [34,56,57]. In our study, we found that treatment of GSP results in an increase in Bax/Bcl-2 ratio in JB6 C141 cells (Figure 7), increased release of cytochrome *c*, activation of Apaf-1 and caspase-9, and, finally, increased expression of cleaved caspase 3 (Figure 8), which may result in increased apoptosis in JB6 C141 cells. Similarly, treatment of GSP to p53$^{+/+}$ cells also results in several-fold increases in Bax/Bcl-2 protein ratio, which may be responsible for making these cells more susceptible for undergoing apoptosis, but this effect was not observed in p53-deficient (p53$^{-/-}$) cells (Figure 9). These results provide evidence for the importance of p53 and its phosphorylation product in GSP-induced apoptosis. At the highest GSP dose levels, a small degree of apoptosis was observed even in the p53$^{-/-}$ cells. Although we do not have experimental evidence to indicate that

this is the case, it is possible that downregulation of Bcl-xl could be responsible for the mild apoptosis observed in the $p53^{-/-}$ cells.

In conclusion, the data from our study indicate for the first time that GSP-induced apoptosis in JB6 C141 cells occurs primarily through a p53-dependent pathway and involves its target proteins of the Bcl-2 family (i.e., Bax, Bcl-2) and activation of caspase 3. Therefore, these findings suggest that tumors retaining wild-type p53 will be more susceptible to chemoprevention with GSP than tumors that express the *p53* mutants. In most human cancers, the p53 is mutated or nonfunctional. In such scenario, GSP may not be beneficial as a chemopreventive agent; however, it may be the possibility that other apoptotic pathways may be involved with the GSP treatment. This remains to be found out. Further, it would prove beneficial to complement GSP with those chemopreventive agents that are insensitive to p53 expression when p53 is absent or mutated. However, our data suggest that GSP have the potential to be developed as a pharmacologically safe agent to prevent cancer.

Acknowledgements

We would also like to gratefully acknowledge Lawrence A. Donehower (Division of Molecular Virology, Baylor College of Medicine, Houston, TX) for the generous gift of $p53^{+/+}$ and $p53^{-/-}$ fibroblasts, and Nancy Colburn (National Cancer Institute, NIH) for JB6 C141 cells.

References

[1] Silva RC, Cheynier V, and Chemina A (1991). Procyanidin dimers and trimers from grape seeds. *Phytochemistry* **30,** 1259–1264.

[2] Prieur C, Rigaud J, Cheynier V, and Moutounet M (1994). Oligomeric and polymeric procyanidins from grape seeds. *Phytochemistry* **36,** 781–789.

[3] Joshi SS, Kuszynski CA, and Bagchi D (2001). The cellular and molecular basis of health benefits of grape seed proanthocyanidin extract. *Curr Pharm Biotechnol* **2,** 187–200.

[4] Uchida S (1980). Condensed tannins scavenging active oxygen radicals. *Med Sci Res* **15,** 831–832.

[5] Shi J, Yu J, Pohorly J, and Kakuda Y (2003). Polyphenolics in grape seeds—biochemistry and functionality. *J Med Food* **6,** 291–299.

[6] Mittal A, Elmets CA, and Katiyar SK (2003). Dietary feeding of proanthocyanidins from grape seeds prevents photocarcinogenesis in SKH-1 hairless mice: relationship to decreased fat and lipid peroxidation. *Carcinogenesis* **24,** 1379–1388.

[7] Agarwal C, Singh RP, Dhanalakshmi S, and Agarwal R (2004). Anti-angiogenic efficacy of grape seed extract in endothelial cells. *Oncol Rep* **11,** 681–685.

[8] Singh RP, Tyagi AK, Dhanalakshmi S, Agarwal R, and Agarwal C (2004). Grape seed extract inhibits advanced human prostate tumor growth and angiogenesis and upregulates insulin-like growth factor binding protein-3. *Int J Cancer* **108,** 733–740.

[9] Vayalil PK, Mittal A, and Katiyar SK (2004). Proanthocyanidins from grape seeds inhibit expression of matrix metalloproteinases in human prostate carcinoma cells, which is associated with the inhibition of activation of MAPK and NFκB. *Carcinogenesis* **25,** 987–995.

[10] Bagchi D, Bagchi M, Stohs S, Ray SD, Sen CK, and Preuss HG (2002). Cellular protection with proanthocyanidins derived from grape seeds. *Ann NY Acad Sci* **957,** 260–270.

[11] Tyagi A, Agarwal R, and Agarwal C (2003). Grape seed extract inhibits EGF-induced and constitutively active mitogenic signaling but activates JNK in human prostate carcinoma DU145 cells: possible role in antiproliferation and apoptosis. *Oncogene* **22,** 1302–1316.

[12] Sharma G, Tyagi AK, Singh RP, Chan DC, and Agarwal R (2004). Synergistic anti-cancer effects of grape seed extract and conventional cytotoxic agent Doxorubicin against human breast carcinoma cells. *Breast Cancer Res Treat* **85,** 1–12.

[13] Ye X, Krohn RL, Liu W, Joshi SS, Kuszynski CA, McGinn TR, Bagchi M, Preuss HG, Stohs SJ, and Bagchi D (1999). The cytotoxic effects of a novel IH636 grape seed proanthocyanidin extract on cultured human cancer cells. *Mol Cell Biochem* **196,** 99–108.

[14] Zhao J, Wang J, Chen Y, and Agarwal R (1999). Anti–tumor-promoting activity of a polyphenolic fraction isolated from grape seeds in the mouse skin two-stage initiation–promotion protocol and identification of procyanidin B5-3′-gallate as the most effective antioxidant constituent. *Carcinogenesis* **20,** 1737–1745.

[15] Finlay CA, Hinds PW, and Levine AJ (1989). The *p53* proto-oncogene can act as a suppressor of transformation. *Cell* **57,** 1083–1093.

[16] Kastan MB, Onyekwere O, Sidransky D, Vogelstein B, and Craig RW (1991). Participation of p53 protein in the cellular response to DNA damage. *Cancer Res* **51,** 6304–6311.

[17] Sherr CJ (2004). Principles of tumor suppression. *Cell* **116,** 235–246.

[18] Bagchi M, Kuszynski CA, Balmoori J, Joshi SS, Stohs SJ, and Bagchi D (2001). Protective effects of antioxidants against smokeless tobacco–induced oxidative stress and modulation of *Bcl-2* and *p53* genes in human oral keratinocytes. *Free Radic Res* **35,** 181–194.

[19] Oltvai ZN, Milliman CL, and Korsmeyer SJ (1993). Bcl-2 heterodimerizes *in vivo* with a conserved homolog, Bax, that accelerates programmed cell death. *Cell* **74,** 609–619.

[20] Marzo I, Brenner C, Zamzami N, Jurgensmeier JM, Susin SA, Vieira HL, Prevost MC, Xie Z, Matsuyama S, Reed JC, and Kroemer G (1998). Bax and adenine nucleotide translocator cooperate in the mitochondrial control of apoptosis. *Science (Washington, DC)* **281,** 2027–2031.

[21] Wang X (2001). The expanding role of mitochondria in apoptosis. *Genes Dev* **15,** 2922–2933.

[22] Colburn NH, Former BF, Nelson KA, and Yuspa SH (1979). Tumor promoter induces anchorage independence irreversibly. *Nature (London)* **281,** 589–591.

[23] Colburn NH, Smith BM, Wendel EJ, Dowjat WK, and Shimada T (1988). Transfer of *pro gene* transfection of tumor promoter–sensitive phenotype to promotion-insensitive JB6 cells. *Cancer Res* **48,** 1195–1200.

[24] Huang C, Ma W, Goranson A, and Dong Z (1999). Resveratrol suppresses cell transformation and induces apoptosis through a p53-dependent pathway. *Carcinogenesis* **20,** 237–242.

[25] He Z, Ma W-Y, Hashimoto T, Bode AM, Yang CS, and Dong Z (2003). Induction of apoptosis by caffeine is mediated by the p53, Bax, and caspase 3 pathways. *Cancer Res* **63,** 4396–4401.

[26] Mosmann T (1983). Rapid colorimetric assay for cellular growth and survival: application to proliferation and cytotoxicity assays. *J Immunol Methods* **65,** 55–63.

[27] Mittal A, Pate MS, Wylie RC, Tollefsbol TO, and Katiyar SK (2004). EGCG down-regulates telomerase in human breast carcinoma MCF-7 cells, leading to suppression of cell viability and induction of apoptosis. *Int J Oncol* **24,** 703–710.

[28] Katiyar SK, Afaq F, Azizuddin K, and Mukhtar H (2001). Inhibition of UVB-induced oxidative stress–mediated phosphorylation of mitogen-activated protein kinase signaling pathways in cultured human epidermal keratinocytes by green tea polyphenol (−)-epigallocatechin-3-gallate. *Toxicol Appl Pharmacol* **176,** 110–117.

[29] Dumaz N and Meek DW (1999). Serine 15 phosphorylation stimulates p53 transactivation but does not directly influence interaction with HDM2. *EMBO J* **18,** 7002–7010.

[30] Larsen CJ (1994). The *BCL2* gene, prototype of a gene family that controls programmed cell death (apoptosis). *Ann Genet* **37,** 121–134 (in French).

[31] Zhan Q, Fan S, Bae I, Guillouf C, Liebermann DA, O'Connor PM, and Fornace AJ Jr (1994). Induction of bax by genotoxic stress in human cells correlates with normal p53 status and apoptosis. *Oncogene* **9,** 3743–3751.

[32] Yang J, Liu X, Bhalla K, Kim CN, Ibrado AM, Cai J, Peng TI, Jones DP, and Wang X (1997). Prevention of apoptosis by Bcl-2: release of cytochrome *c* from mitochondria blocked. *Science (Washington, DC)* **275,** 1129–1132.

[33] Liu X, Kim CN, Yang J, Jemmerson R, and Wang X (1996). Induction of apoptotic program in cell-free extracts: requirement for dATP and cytochrome *c*. *Cell* **86,** 147–157.

[34] Kluck RM, Bossy-Wetzel E, Green DR, and Newmeyer DD (1997). The release of cytochrome *c* from mitochondria: a primary site for Bcl-2 regulation of apoptosis. *Science (Washington, DC)* **275,** 1132–1136

[35] Bomser JA, Singletary KW, Wallig MA, and Smith MA (1999). Inhibition of TPA-induced tumor promotion in CD-1 mouse epidermis by a polyphenolic fraction from grape seeds. *Cancer Lett* **135,** 151–157.
[36] Bursch W, Oberhammer F, and Schulte-Hermann R (1992). Cell death by apoptosis and its protective role against disease. *Trends Pharmacol Sci* **13,** 245–251.
[37] Fisher DE (1994). Apoptosis in cancer therapy: crossing the threshold. *Cell* **78,** 539–542.
[38] Wright SC, Zhong J, and Larrick JW (1994). Inhibition of apoptosis as a mechanism of tumor promotion. *FASEB J* **8,** 654–660.
[39] Barry MA, Behnke CA, and Eastmann A (1990). Activation of programmed cell death (apoptosis) by cisplatin, other anticancer drugs, toxins, and hyperthermia. *Biochem Pharmacol* **40,** 2353–2362.
[40] Hickman JA (1992). Apoptosis induced by anticancer drugs. *Cancer Metastasis Rev* **11,** 121–129.
[41] Lowe SW, Jacks T, Housman DE, and Ruley HE (1994). Abrogation of oncogene-associated apoptosis allows transformation of p53-deficient cells. *Proc Natl Acad Sci USA* **91,** 2026–2030.
[42] Symonds H, Krall L, Remington L, Saenz-Robles M, Lowe S, Jacks T, and Van Dyke T (1994). p53-dependent apoptosis suppresses tumor growth and progression *in vivo*. *Cell* **78,** 703–711.
[43] Hollstein M, Rice K, Greenbalt MS, Soussi T, Fuchs R, Sorlie T, Hovig E, Smith-Sorensen B, Montesano R, and Harris CC (1994). Database of *p53* gene somatic mutations in human tumors and cell lines. *Nucleic Acids Res* **22,** 3551–3555.
[44] Donehower LA, Harvey M, Slagle BL, McArthur MJ, Montgomery CA Jr, Butel JS, and Bradley A (1992). Mice deficient for p53 are developmentally normal but susceptible to spontaneous tumors. *Nature* **356,** 215–221.
[45] Komarova EA, Chernov MV, Franks R, Wang K, Armin G, Zelnick CR, Chin DM, Bacus SS, Stark GR, and Gudkov AV (1997). Transgenic mice with p53-responsive lacZ: p53 activity varies dramatically during normal development and determines radiation and drug sensitivity *in vivo*. *EMBO J* **16,** 1391–1400.
[46] Shieh SY, Ikeda M, Taya Y, and Prives C (1997). DNA damage–induced phosphorylation of p53 alleviates inhibition by MDM2. *Cell* **91,** 325–334.
[47] Tibbetts RS, Brumbaugh KM, Williams JM, Sarkaria JN, Cliby WA, Shieh SY, Taya Y, Prives C, and Abraham RT (1999). A role for ATR in the DNA damage–induced phosphorylation of p53. *Genes Dev* **13,** 152–157.
[48] Venkatachalam S, Shi YP, Jones SN, Vogel H, Bradley A, Pinkel D, and Donehower LA (1998). Retention of wild-type p53 in tumors from p53 heterozygous mice: reduction of p53 dosage can promote cancer formation. *EMBO J* **17,** 4657–4667.
[49] Kaina B (2003). DNA damage–triggered apoptosis: critical role of DNA repair, double-strand breaks, cell proliferation and signaling. *Biochem Pharmacol* **66,** 1547–1554.
[50] McCurrach ME, Connor TM, Knudson CM, Korsmeyer SJ, and Lowe SW (1997). Bax-deficiency promotes drug resistance and oncogenic transformation by attenuating p53-dependent apoptosis. *Proc Natl Acad Sci USA* **94,** 2345–2349.
[51] Yin C, Knudson CM, Korsmeyer SJ, and Van Dyke T (1997). Bax suppresses tumorigenesis and stimulates apoptosis *in vivo*. *Nature* **385,** 637–640.
[52] Ryan KM, Phillips AC, and Vousden KH (2001). Regulation and function of the p53 tumor suppressor protein. *Curr Opin Cell Biol* **13,** 332–337.
[53] Donovan M and Cotter TG (2004). Control of mitochondrial integrity by Bcl-2 family members and caspase-independent cell death. *Biochim Biophys Acta* **1644,** 133–147.
[54] Tang DG and Porter AT (1997). Target to apoptosis: a hopeful weapon for prostate cancer. *Prostate* **32,** 284–293.
[55] Ruvolo PP, Deng X, and May WS (2001). Phosphorylation of Bcl-2 and regulation of apoptosis. *Leukemia* **15,** 515–522.
[56] Reed JC (1995). Regulation of apoptosis by Bcl-2 family proteins and its role in cancer and chemoresistance. *Curr Opin Oncol* **7,** 541–546.
[57] Communal C, Sumandea M, de Tombe P, Narula J, Solaro RJ, and Hajjar RJ (2002). Functional consequences of caspase activation in cardiac myocytes. *Proc Natl Acad Sci USA* **99,** 6252–6256.